

Charge-exchange spin monopole modes

I. Hamamoto¹ and H. Sagawa²

¹*Department of Mathematical Physics, Lund Institute of Technology, University of Lund, Lund, Sweden*

²*Center for Mathematical Sciences, University of Aizu, Ikki-machi, Aizu-Wakamatsu, Fukushima 965, Japan*

(Received 27 March 2000; published 25 July 2000)

Using the self-consistent Hartree-Fock plus Tamm-Dancoff approximation with Skyrme interactions, the response of some β stable closed-shell nuclei to charge-exchange (t_{\pm}) spin monopole fields is estimated in the coordinate space. Both the isoscalar and isovector spin-correlation are included simultaneously. The excitation energy of t_{+} giant resonance decreases considerably as the neutron excess (and consequently the nuclear mass number) increases, while that of t_{-} giant resonance remains nearly constant. We have tried to separate out the Gamow-Teller strength from the present charge-exchange spin monopole strength, both of which have the same quantum numbers, $J^{\pi}=1^{+}$.

PACS number(s): 21.60.Jz, 23.20.Js, 25.40.Kv

I. INTRODUCTION

Including simultaneously both the isoscalar (IS) and isovector (IV) spin correlation, the response function of the self-consistent random phase approximation (RPA) based on Hartree-Fock (HF) calculations to spin-dependent fields is studied in light drip line nuclei in Ref. [1]. The estimate is made in the coordinate space using the Green's function method so as to take properly into account the continuum effect. Using the same kind of technique as in Ref. [1] but employing the Tamm-Dancoff approximation (TDA) rather than RPA, in the present work we study the response to the charge-exchange spin monopole fields. The external operator has the same quantum number $J^{\pi}=1^{+}$ as the Gamow-Teller (GT) operator, though the excitation mode is compression mode, of which the transition density has a radial node. Thus, we try to separate the GT strength from the estimated response to the charge-exchange spin monopole field.

It is stated in Ref. [2] that in order to excite efficiently a compression mode one needs a strongly absorbed projectile which will not penetrate deeply into the nucleus and will not probe the entire volume part of the transition density. The (π^{\pm}, π_0) reactions with the energy around (3,3) resonance may be such a reaction appropriate for populating the isovector compression modes. When the spin degree of freedom is further involved in the mode, the simplest example of which is the isovector spin monopole (IVSM) resonance, the reactions such as ($^3\text{He}, t$) or (p, n) with carefully chosen incident energies would be appropriate for the population. Indeed, in Ref. [2] the IVSM mode is calculated and the population of it is suggested as an interpretation of the observed rather large background spectra around $E_x=30$ MeV of ^{90}Nb at the forward angle in the $^{90}\text{Zr}(^3\text{He}, t)^{90}\text{Nb}$ reaction at $E_{\text{lab}}=600$ MeV. On the other hand, in Ref. [3] the contribution to the $L=0$ cross section in the (p, n) reaction with $T_p=295$ MeV by the IVSM modes is estimated and subtracted in order to obtain the total GT strength summed over the region up to 50 MeV excitation. In Ref. [4] Auerbach discusses various conditions of observing isovector (spin-flip or spin-independent) giant monopole resonances.

The calculation of the IVSM response in ^{90}Zr presented in Ref. [2] was not performed by using the same Skyrme interaction in both HF and RPA. Moreover, the GT strength

which may be found in the same energy region may affect considerably the calculated IVSM response, since the former was not explicitly subtracted in Ref. [2]. The inclusion of small amplitudes of the GT response can appreciably change the IVSM strength function, when the total amplitudes are squared. In the present paper we propose a way of eliminating efficiently the GT strength from the IVSM response so that we can discuss the pure IVSM response as well as the GT strength remaining in the high-energy region. The main aim of the present work is to study the dependence of the properties of t_{\pm} spin monopole modes on neutron excess and mass-number. Since the pair correlation is not included in the present work, we study the closed-shell nuclei $^{48}_{20}\text{Ca}_{28}$, $^{90}_{40}\text{Zr}_{50}$, and $^{208}_{82}\text{Pb}_{126}$.

In Sec. II the model and necessary formulas are described, while in Sec. III numerical results and discussions are presented. In Sec. IV the conclusion is given.

II. MODEL AND FORMULAS

We perform the self-consistent HF plus TDA calculations using Skyrme interactions. The TDA equations are solved in the coordinate space so as to take into account properly the coupling to the continuum. Both the IS and IV spin correlations are included simultaneously. The reason why we use TDA instead of RPA is that in the calculation of charge-exchange modes based on the ground state of mother nuclei the response function below the ground state cannot be estimated by RPA, since the energy of the solution becomes imaginary. The particle-hole (p - h) interaction is derived from the Hamiltonian of Skyrme interactions by so-called Landau procedure and is given in Ref. [1].

The operator of the external field for the IVSM modes used in the literature is defined as

$$O_{1\mu}^{\pm} = \sum_i t_{\pm}(i) \sigma_{\mu}(i) r(i)^2 \quad (1)$$

which is compared with the GT operator

$$GT_{1\mu}^{\pm} = \sum_i t_{\pm}(i) \sigma_{\mu}(i). \quad (2)$$

Since both operators, Eqs. (1) and (2), have the same quantum numbers $J^\pi = 1^+$, the response function to the operator (1) naturally accommodates also the possible GT strength, though the major part of GT strength appears in the region of much lower energy. The spin transition density is defined as

$$\delta\rho_\mu^\pm(\vec{r}) = \sum_i \langle n | t_\pm(i) \sigma_\mu(i) \delta(\vec{r} - \vec{r}(i)) | 0 \rangle. \quad (3)$$

In order to eliminate the GT strength, we use the operator for the t_- IVSM modes

$$SM_{1\mu}^- = \sum_i t_-(i) \sigma_\mu(i) [r(i)^2 - \langle r^2 \rangle_{\text{excess}}] \quad (4)$$

for the nuclei with neutron excess studied, while we employ for the t_+ IVSM modes either

$$SM_{1\mu}^+ = \sum_i t_+(i) \sigma_\mu(i) [r(i)^2 - \langle r^2 \rangle_{\text{excess}}] \quad (5)$$

or $O_{1\mu}^+$ in (1). In Eq. (4) the average value of $\langle r^2 \rangle$ for the excess neutrons is expressed by $\langle r^2 \rangle_{\text{excess}}$. In the construction of the operator in Eq. (4) we have used the approximation that the radial dependence of the wave functions of proton orbitals, which are populated by the GT^- operator acting on the excess neutrons, is the same as that of the excess-neutron orbitals. For the t_+ IVSM modes the response functions would be the same for the operator $SM_{1\mu}^+$ and $O_{1\mu}^+$, if the t_+ GT strength is absent in the nucleus. In the closed-shell nuclei studied in the present work the t_+ GT strength is absent if the radial wave functions of neutrons and protons with the same quantum numbers (n, l, j) are the same. Thus, the magnitude of possible nonvanishing t_+ GT strength in those nuclei can be exhibited by the difference of the calculated response functions for the operators $SM_{1\mu}^+$ and $O_{1\mu}^+$.

The strength function for the operator $SM_{1\mu}$ is defined as

$$S(E) \equiv \sum_n |\langle n | SM_{1\mu} | 0 \rangle|^2 \delta(E - E_n). \quad (6)$$

Defining

$$S_-^{(O)} \equiv \sum_\mu \sum_n |\langle n | t_- \sigma_\mu r^2 | 0 \rangle|^2 \quad (7)$$

and

$$S_+^{(O)} \equiv \sum_\mu \sum_n |\langle n | t_+ \sigma_\mu r^2 | 0 \rangle|^2, \quad (8)$$

the non-energy-weighted sum rule is obtained as

$$S_-^{(O)} - S_+^{(O)} = 3[N\langle r^4 \rangle_n - Z\langle r^4 \rangle_p], \quad (9)$$

which contains in principle the contribution by the GT strength. On the other hand, defining

$$S_-^{(\text{SM})} \equiv \sum_\mu \sum_n |\langle n | t_- \sigma_\mu (r^2 - \langle r^2 \rangle_{\text{excess}}) | 0 \rangle|^2 \quad (10)$$

and

$$S_+^{(\text{SM})} \equiv \sum_\mu \sum_n |\langle n | t_+ \sigma_\mu (r^2 - \langle r^2 \rangle_{\text{excess}}) | 0 \rangle|^2, \quad (11)$$

the non-energy-weighted sum rule is obtained as

$$S_-^{(\text{SM})} - S_+^{(\text{SM})} = 3[N\langle r^4 \rangle_n - Z\langle r^4 \rangle_p - 2\langle r^2 \rangle_{\text{excess}} \\ \times (N\langle r^2 \rangle_n - Z\langle r^2 \rangle_p) + \langle r^2 \rangle_{\text{excess}}^2 (N - Z)] \quad (12)$$

$$= \begin{cases} 1880 & \text{fm}^4 \text{ for } {}^{48}\text{Ca}, \\ 3524 & \text{fm}^4 \text{ for } {}^{90}\text{Zr}, \\ 47560 & \text{fm}^4 \text{ for } {}^{208}\text{Pb}. \end{cases} \quad (13)$$

The values of Eq. (13) are estimated by using the HF states with the SGII interaction.

III. NUMERICAL RESULTS AND DISCUSSIONS

Among Skyrme interactions available in the literature we choose to show the numerical results with the SGII interaction, which has an acceptable value of the incompressibility of nuclear matter $K_{\text{NM}} = 215$ MeV, and which is effectively repulsive not only in the $(\vec{\sigma} \cdot \vec{\sigma})(\vec{\tau} \cdot \vec{\tau})$ channel but also in the $(\vec{\sigma} \cdot \vec{\sigma})$ channel [5]. Those properties of the SGII interaction may play an important role in the estimated result of charge-exchange spin monopole modes.

In Fig. 1 we show the unperturbed and TDA IVSM strength function of ${}^{48}\text{Ca}_{28}$, ${}^{90}\text{Zr}_{50}$, and ${}^{208}\text{Pb}_{126}$, respectively, using the operators (4) and (5). Only the strength above the calculated threshold is plotted in both the unperturbed and TDA case, since the strength of the excitations from the bound to bound state has a different dimension. The values of $\langle r^2 \rangle_{\text{excess}}$ used for ${}^{48}\text{Ca}$, ${}^{90}\text{Zr}$, and ${}^{208}\text{Pb}$ are 16.71, 23.65, and 36.76 fm², respectively. The peak position and shape of the calculated t_- TDA response of ${}^{90}\text{Zr}$ exhibited in Fig. 1(b) are qualitatively similar to those shown in Fig. 2 of Ref. [2], which were calculated using the operator (1) and an RPA with a different interaction. See also Ref. [6]. The sharp peak at 20.6 MeV of the t_- TDA of ${}^{208}\text{Pb}$ in Fig. 1(c) is in fact the GT strength coming from the $(1i_{13/2})_n \rightarrow (1i_{11/2})_p$ excitation, which is difficult to be completely eliminated by using the operator (4) due to the exceptionally large value of the radial matrix element $\langle (1i_{11/2})_p | r^2 | (1i_{13/2})_n \rangle$. The sum-rule values (10) and (11), for our TDA response are shown in Table I. The calculated strength summed up till $E_x = 70$ MeV becomes 96.4, 97.3, and 100.7 % of the values in Eq. (13) for ${}^{48}\text{Ca}$, ${}^{90}\text{Zr}$, and ${}^{208}\text{Pb}$, respectively.

Defining the energy moment of transition strength

$$m_k^\pm \equiv \sum_n (E_n)^k |\langle n | SM_{1\mu}^\pm | 0 \rangle|^2, \quad (14)$$

we obtain the averaged energies of IVSM giant resonances

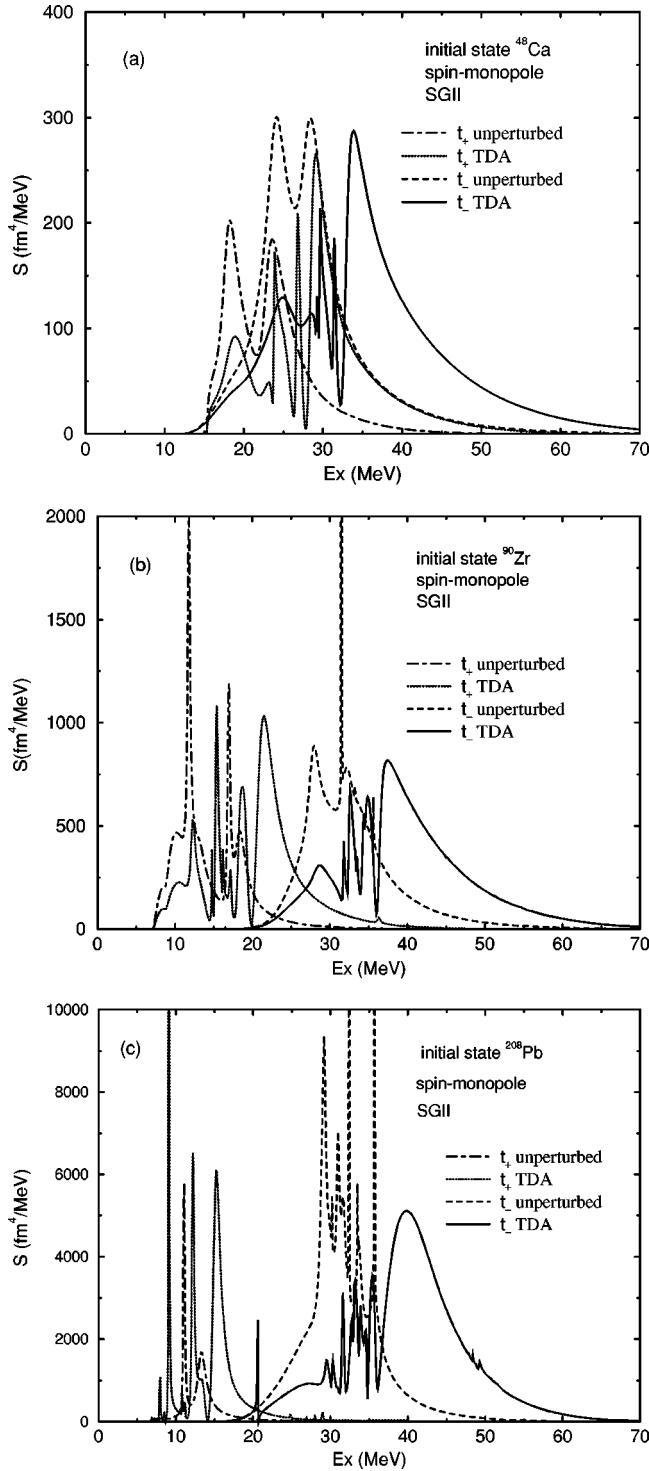


FIG. 1. Unperturbed and TDA response function to the operators (4) and (5), for (a) ${}^{48}\text{Ca}_{28}$, (b) ${}^{90}\text{Zr}_{50}$, and (c) ${}^{208}\text{Pb}_{126}$. The energy plotted on the x axis is measured from the ground state of mother nuclei. The energy measured from the ground state of daughter nuclei is obtained by subtracting the respective binding-energy difference, Eq. (16) for t_- modes and Eq. (17) for t_+ modes, from the energy indicated on the x axis. The SGII interaction is used both in the HF and TDA calculations.

TABLE I. Integrated sum rule values (10) and (11) of TDA response to the operators (4) and (5). The TDA strength is integrated up to $E_x = 70$ MeV. The SGII interaction is used.

	$S_-^{(SM)}$ (fm ⁴)	$S_+^{(SM)}$ (fm ⁴)	$S_-^{(SM)} - S_+^{(SM)}$ (fm ⁴)
${}^{48}\text{Ca}$	4.02×10^3	2.21×10^3	1.81×10^3
${}^{90}\text{Zr}$	1.21×10^3	7.74×10^3	3.43×10^3
${}^{208}\text{Pb}$	6.90×10^4	2.11×10^4	4.79×10^4

$$E_{\pm} = \frac{m_1^{\pm}}{m_0^{\pm}} \quad (15)$$

which are tabulated in Table II, where for reference we also show the calculated averaged energies obtained by using the SIII interaction. It is seen that the value of E_+ for the SGII interaction is about 2 MeV systematically lower than that for the SIII interaction, while the E_- value for the SGII interaction is slightly higher than that for the SIII interaction. The systematic difference of the E_{\pm} values for the SGII and SIII interaction is seen already in respective unperturbed energies. The spin-orbit splitting obtained by using the SGII and SIII interaction is nearly the same. However, there is a general tendency that for bound neutrons one-particle orbitals around the Fermi level which are estimated with the SGII interaction are more bound than those with the SIII interaction, while for bound protons the formers are less bound than the latters. Consequently, for example, in ${}^{208}\text{Pb}$ the unperturbed energies of $N_p = 4 \rightarrow N_n = 6$ (t_+) excitations for the SGII interaction are appreciably lower than those for the SIII interaction, while those of $N_n = 5 \rightarrow N_p = 5$ (t_-) excitations for the SGII interaction are higher than those for the SIII interaction. However, for the t_- IVSM mode the major unperturbed excitations are from the $N_n = 5$ and 4 shell to the $N_p = 7$ and 6 shell, respectively. Those $\Delta N = 2$ (t_-) unperturbed excitation energies are in fact nearly the same for the SGII and SIII interaction.

In Fig. 2 the radial part of the TDA transition density of ${}^{208}\text{Pb}$ is exhibited for the t_- mode calculated at 39.8 MeV and the t_+ mode at 15.3 MeV, respectively. Those energies are chosen, in which we expect to have the collective transition density of respective IVSM modes in the present numerical calculation. The transition densities have a radial node expressing that the modes are compression modes. The position of the radial node for the t_+ mode lies more inside than that for the t_- mode, reflecting the fact that the t_+ mode

TABLE II. Average energy of IVSM giant resonances defined in Eq. (15), calculated by using the SGII and SIII interactions.

	SGII		SIII	
	E_- (MeV)	E_+ (MeV)	E_- (MeV)	E_+ (MeV)
${}^{48}\text{Ca}$	35.7	29.6	35.2	31.5
${}^{90}\text{Zr}$	40.0	20.8	39.6	22.1
${}^{208}\text{Pb}$	39.9	14.3	38.3	16.5

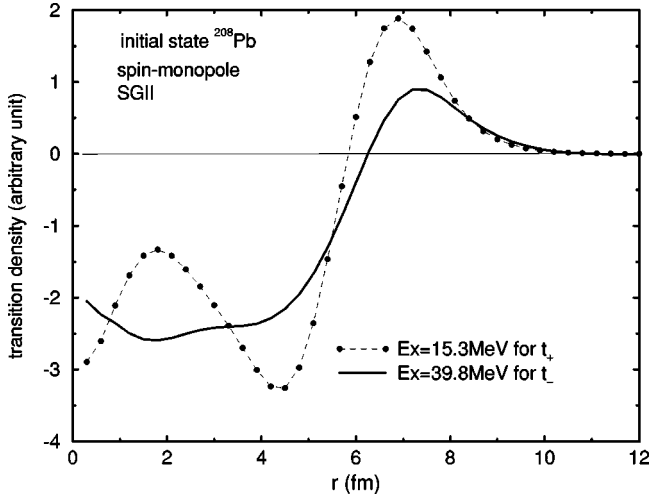


FIG. 2. Radial part of TDA spin transition densities (3) of $^{208}_{82}\text{Pb}_{126}$ in arbitrary units, which are calculated at 39.8 MeV for the t_- mode and at 15.3 MeV for the t_+ mode, respectively.

is energetically lower lying. The structure of transition densities inside the nuclei comes from the detailed shell structure of constituent p - h configurations.

The fact that the calculated TDA result is understood in terms of unperturbed excitation energies shows that the collective correlation effect relevant to the IVSM modes is similar for the SGII and SIII interaction. It is seen that the large difference of the nuclear matter incompressibility of the SGII and SIII interaction plays little role in the present IVSM modes, which are the isovector compression modes. Since the experimental data, to which the parameters of Skyrme interactions are fitted, are not sensitive to the isovector incompressibility, there may be non-negligible ambiguity in the calculated properties of IVSM modes. In other words, possible experimental information on charge-exchange IVSM modes can pin down an important parameter of effective interactions.

In Fig. 3 the t_+ IVSM strength functions of ^{90}Zr obtained by using the operators $SM_{1\mu}^+$ and $O_{1\mu}^+$ are compared. The possible difference between the two strength functions indicates the presence of t_+ GT strength in the energy region. It is seen that a small amount of t_+ GT strength remains in both the low and high energy region. The GT strength comes from the small difference of the neutron and proton one-particle wave-functions with the same quantum numbers (n, j, l) . In the whole energy region the strength for the operator $SM_{1\mu}^+$ is appreciably smaller than that for $O_{1\mu}^+$.

In Fig. 4 the t_- IVSM strength functions of ^{90}Zr obtained by using the operators $SM_{1\mu}^-$ and $O_{1\mu}^-$ are compared. The two sharp peaks at $Ex = 8.44$ and 16.51 MeV in Fig. 4 originating from the unperturbed excitations $(1g_{9/2})_n \rightarrow (1g_{9/2})_p$ and $(1g_{9/2})_n \rightarrow (1g_{7/2})_p$, are almost pure GT strength. The position of the GT peak at $Ex = 8.44$ MeV is indicated, though the peak lies below the threshold and thus has a different dimension. In the whole energy region of $Ex \geq 20$ MeV one may identify the presence of t_- GT strength, recognizing that the strength for the operator $SM_{1\mu}^-$ is appreciably larger than that for $O_{1\mu}^-$. The constructive and de-

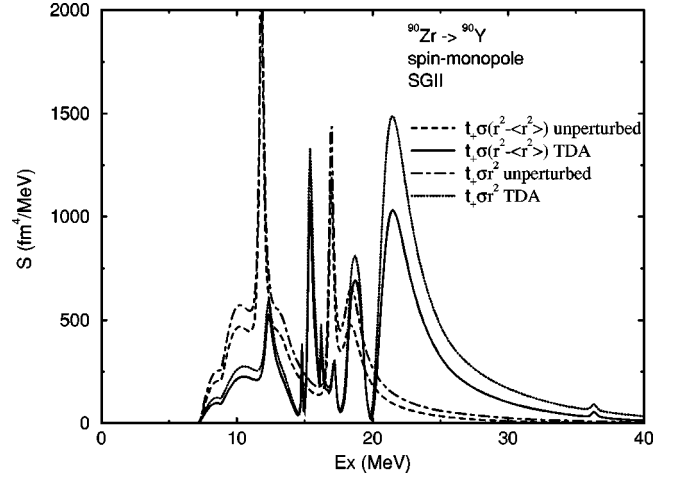


FIG. 3. Comparison between the t_+ TDA response function of ^{90}Zr to the operator $SM_{1\mu}^+$ in Eq. (5) and that to $O_{1\mu}^+$ in Eq. (1). The possible difference between the two response functions at a given energy indicates the presence of t_+ GT strength in the energy region. The energy plotted on the x axis is measured from the ground state of mother nuclei.

structive relation between the radial matrix elements of r^2 and $-\langle r^2 \rangle$ for the t_- and t_+ case, respectively, come from the fact that for the same quantum-numbers (n, l, j) the proton one-particle radial wave-function is slightly more extended than the neutron one.

Since in numerical calculations the response functions of charge exchange modes are estimated based on the ground states of mother nuclei, the strength functions in Figs. 1, 3, and 4 are plotted as a function of the energy measured from the ground state of mother nuclei. However, it may be more appropriate to express the calculated strength function as a function of excitation energy of daughter nuclei. The energy difference between the ground states of the mother and

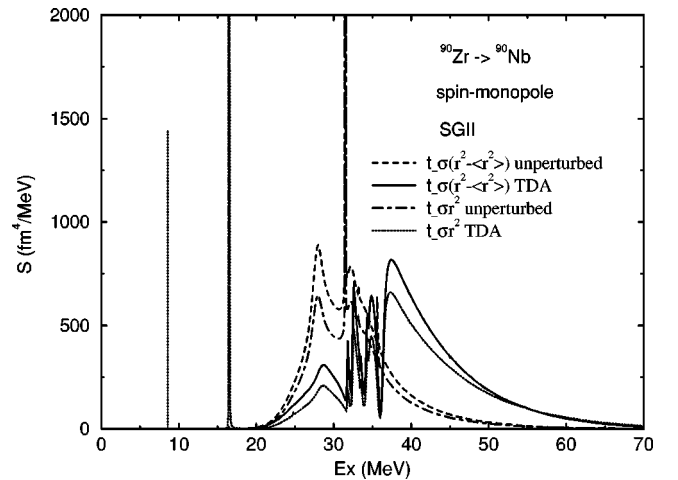


FIG. 4. Comparison between the t_- TDA response function of ^{90}Zr to the operator $SM_{1\mu}^-$ in Eq. (4) and that to $O_{1\mu}^-$ in Eq. (1). The position of the GT peak at 8.44 MeV is indicated for reference, though the peak lies below the threshold and thus has a different dimension. The energy plotted on the x axis is measured from the ground state of mother nuclei.

daughter nuclei is equal to the difference of the binding energies of respective nuclei. In the closed shell nuclei studied we find in the mass table [7]

$$\begin{aligned} B(^{48}_{20}\text{Ca}_{28}) - B(^{48}_{21}\text{Sc}_{27}) &= 0.504 \text{ MeV}, \\ B(^{90}_{40}\text{Zr}_{50}) - B(^{90}_{41}\text{Nb}_{49}) &= 6.893 \text{ MeV}, \\ B(^{208}_{82}\text{Pb}_{126}) - B(^{208}_{83}\text{Bi}_{125}) &= 3.661 \text{ MeV} \end{aligned} \quad (16)$$

for t_- modes, while

$$\begin{aligned} B(^{48}_{20}\text{Ca}_{28}) - B(^{48}_{19}\text{K}_{29}) &= 11.308 \text{ MeV}, \\ B(^{90}_{40}\text{Zr}_{50}) - B(^{90}_{39}\text{Y}_{51}) &= 1.499 \text{ MeV}, \\ B(^{208}_{82}\text{Pb}_{126}) - B(^{208}_{81}\text{Tl}_{127}) &= 4.219 \text{ MeV} \end{aligned} \quad (17)$$

for t_+ modes. The strong variation of the binding-energy differences in Eqs. (16) and (17) comes from the fact that the nucleus ^{48}Ca (^{90}Zr) lies on the neutron-rich (proton-rich) side of the β stable isotope with $Z=20$ ($Z=40$), while ^{208}Pb lies near the center of the isotope with $Z=82$.

We have obtained the clear tendency that in the β stable nuclei the average peak energy of the t_+ IVSM giant resonance measured from the ground state of mother nuclei decreases sharply as the mass number increases, while that of the t_- IVSM giant resonance remains nearly independent of the mass number. We understand this tendency already in the energy of unperturbed p - h excitations in the following way, partly using the harmonic oscillator model, of which the principal quantum number of the last-filled major shell for neutrons and protons is expressed by N_F^n and N_F^p , respectively. First of all, we notice that along the β stability line the difference of the number of neutrons and protons is approximately expressed [8] by

$$(N - Z)_{\beta\text{-stable}} \approx 6 \times 10^{-3} A^{5/3}, \quad (18)$$

which is obtained by minimizing the total mass for the fixed mass number A . Then, using the relations such as

$$\frac{1}{3}(N_F^n + 2)^3 = N \quad \text{and} \quad \frac{1}{3}(N_F^p + 2)^3 = Z, \quad (19)$$

which are valid for $N_F^n \gg 1$ and $N_F^p \gg 1$, we obtain

$$(N_F^n - N_F^p) = 6 \left(\frac{2}{3} \right)^{2/3} 10^{-3} A = 0.0046 A. \quad (20)$$

On the other hand, in β stable nuclei the separation energy of neutrons is nearly equal to that of protons, namely, neutrons in the N_F^n shell have nearly the same separation energy as that of protons in the N_F^p shell. Then, taking $2\hbar\omega_0$ ($= 80A^{-1/3}$ MeV) for the excitation energy of the operator r^2 in IVSM modes and adjusting the energy difference of the neutron and proton last-filled major shell $(N_F^n - N_F^p)\hbar\omega_0 = 0.183A^{2/3}$ MeV, we obtain

$$(80A^{-1/3} \mp 0.183A^{2/3}) \text{ MeV for the } t_{\pm} \text{ mode} \quad (21)$$

for the p - h excitation energy of charge-exchange IVSM modes measured from the ground state of mother nuclei. The relative strength of the first and second terms in Eq. (21) is such that as the mass number A increases from 90 to 208, the decrease of the first term is compensated by the increase of the second term in the case of the t_- mode. In the case of the t_+ mode the excitation energy expressed in Eq. (21) decreases monotonically as A increases. Typical unperturbed p - h excitation energies for the operators (4) and (5) obtained in our HF calculations, which can be read from Fig. 1, are appreciably larger than those given by the estimate in the schematic model (21). Nevertheless, the qualitative features of our numerical result are well understood by the expression (21).

IV. CONCLUSION

The self-consistent HF plus TDA response function with Skyrme interactions to the charge-exchange spin monopole fields is estimated in the coordinate space, including simultaneously both the IS and IV spin correlation. Numerical result of some β stable closed-shell nuclei using the SGII interaction is presented. The SGII interaction is chosen, since it has the value of incompressibility widely accepted and since it is effectively repulsive not only in the $(\vec{\sigma} \cdot \vec{\sigma})(\vec{\tau} \cdot \vec{\tau})$ channel but also in the $(\vec{\sigma} \cdot \vec{\sigma})$ channel. However, since the so-called nuclear-matter incompressibility is the isoscalar incompressibility, we find that it does not affect so much the correlation relevant to the present IVSM modes. In other words, the possible observation of IVSM modes is a nice way to obtain the information on the isovector incompressibility. The t_+ IVSM giant resonance may be easier to be found in heavier nuclei such as ^{208}Pb , since it is expected to lie energetically lower.

Using the operator $SM_{1\mu}^-$ in Eq. (4), we try to eliminate the possible admixture of t_- GT strength into the t_- IVSM strength. On the other hand, using two kinds of operators, $SM_{1\mu}^+$ and $O_{1\mu}^+$, to evaluate the t_+ IVSM strength, we identify the small portion of the t_+ GT strength present in those closed-shell nuclei, which is absent in the zeroth order approximation. The nonvanishing t_{\pm} GT strength for the nucleus ^{90}Zr is indeed found in the whole energy region. In the energy region where IVSM strength is appreciable the $SM_{1\mu}^+$ strength is weaker than the $O_{1\mu}^+$ strength, while the $SM_{1\mu}^-$ strength is stronger than the $O_{1\mu}^-$ strength. The excitation energy of t_+ IVSM giant resonance decreases drastically as the neutron excess (and the mass number) increases, while that of t_- giant resonance remains almost unchanged independently of mass number.

ACKNOWLEDGMENTS

The authors are grateful to Professor H. Sakai for drawing their attention to the subject of charge-exchange spin monopole giant resonance.

- [1] I. Hamamoto and H. Sagawa, Phys. Rev. C **60**, 064314 (1999).
- [2] N. Auerbach, F. Osterfeld, and T. Udagawa, Phys. Lett. B **219**, 184 (1989).
- [3] H. Sakai *et al.*, Nucl. Phys. **A649**, 251c (1999).
- [4] N. Auerbach, Comments Nucl. Part. Phys. **22**, 223 (1998).
- [5] N. Van Giai and H. Sagawa, Phys. Lett. **106B**, 379 (1981).
- [6] N. Auerbach and A. Klein, Phys. Rev. C **30**, 1032 (1984).
- [7] G. Audi and A. H. Wapstra, Nucl. Phys. **A565**, 1 (1993).
- [8] A. Bohr and B. R. Mottelson, *Nuclear Structure* (Benjamin, Reading, MA, 1969), Vol. I, Chap. 2.